

Cite this: *Chem. Sci.*, 2020, 11, 551

All publication charges for this article have been paid for by the Royal Society of Chemistry

Received 7th October 2019  
Accepted 23rd November 2019

DOI: 10.1039/c9sc05026d

rsc.li/chemical-science

# Reduction of a dihydroboryl cation to a boryl anion and its air-stable, neutral hydroboryl radical through hydrogen shuttling†

Stephan Hagspiel,<sup>ab</sup> Merle Arrowsmith,<sup>ab</sup> Felipe Fantuzzi,<sup>ab</sup> Alexander Hermann,<sup>ab</sup> Valerie Paprocki,<sup>ab</sup> Regina Drescher,<sup>ab</sup> Ivo Krummenacher<sup>ab</sup> and Holger Braunschweig<sup>ab</sup>

The addition of Lewis bases to a cyclic (alkyl)(amino)carbene (CAAC)-supported dihydroboron triflate yields the mixed doubly base-stabilised dihydroboryl cations [(CAAC)BH<sub>2</sub>L]<sup>+</sup>. Of these, [(CAAC)<sub>2</sub>BH<sub>2</sub>]OTf (OTf = triflate) underwent facile two-electron reduction with KC<sub>8</sub> owing to a 1,2-hydride migration from boron to the carbene carbon to yield a stable hydroboryl anion. One-electron oxidation of the latter yielded the first neutral hydroboryl radical, which is bench-stable in the solid state.

## Introduction

Cyclic (alkyl)(amino)carbenes (CAACs) have become the ligands of choice for the stabilisation of many main group compounds in low oxidation states owing to their excellent  $\sigma$ -donor and  $\pi$ -acceptor properties derived from a relatively high-lying HOMO and low-lying LUMO.<sup>1–4</sup> In the field of low-valent mononuclear boron chemistry, they have been successfully employed to synthesise unusual boron(II) species such as boryl radicals [(CAAC)BXY]<sup>•</sup>; X, Y = anionic ligands, e.g. **I**, Fig. 1a),<sup>5–10</sup> boryl radical cations [(CAAC)LBY]<sup>•+</sup>, L = Lewis donor<sup>10–13</sup> and boryl anions [(CAAC)BXY]<sup>–</sup>, e.g. **II**),<sup>14–17</sup> as well as boron(I) species such as borylenes ((CAAC)LBX, e.g. **III**, and (CAAC)BNR<sub>2</sub>).<sup>6–8,11–13,16,18–20</sup> In all these compounds, the accumulation of negative charge on the low-valent boron centre is stabilised through  $\pi$  back-bonding to the CAAC ligand(s) (Fig. 1a), making many of them surprisingly stable under inert conditions.<sup>1–4</sup> Recently, transient dicoordinate (CAAC)-stabilised borylenes have drawn particular attention as compounds capable of activating and catenating N<sub>2</sub>,<sup>21–25</sup> the latter reaction being unprecedented even in transition metal chemistry.

Furthermore, CAACs have been shown to activate element-hydrogen  $\sigma$  bonds, including H–H, N–H, P–H, Si–H and B–H by addition to their nucleophilic carbene carbon.<sup>3,4</sup> In CAAC-

supported hydroboron compounds, the B–H bond activation process can be reversible (Fig. 1b)<sup>14,26,27</sup> and is favoured by electron-donating ligands at boron,<sup>8,26–30</sup> thereby affording additional stabilisation for electron-rich lower oxidation state species through facile hydrogen shuttling. In this contribution we combine the excellent  $\sigma$ -donating/ $\pi$ -accepting and B–H bond activating properties of CAACs to synthesise and isolate a solvent-free alkyl(hydro)boryl anion, and selectively oxidise it to the corresponding radical, which is surprisingly air-stable in the solid state.

## Results and discussion

Following a procedure by Bertrand and co-workers,<sup>12</sup> methyl trifluoromethanesulfonate (MeOTf) was employed to abstract a hydride from (CAAC<sup>Me</sup>)BH<sub>3</sub> (CAAC<sup>Me</sup> = 1-(2,6-diisopropylphenyl)-3,3,5,5-tetramethylpyrrolidin-2-ylidene). The resulting triflate derivative **1** was treated in a 1 : 1 ratio with a series of Lewis bases in benzene to generate the bis(base)-stabilised boronium cations [(CAAC<sup>Me</sup>)BH<sub>2</sub>L]<sup>+</sup>OTf<sup>–</sup> (**2-L**, L = CAAC<sup>Me</sup>, IMe<sup>Me</sup> = 1,3-dimethylimidazol-2-ylidene, PMe<sub>3</sub>, Scheme 1a), all presenting a characteristic upfield <sup>11</sup>B NMR BH<sub>2</sub> triplet in the –22 to –30 ppm region. In the case of the 4-dimethylaminopyridine (DMAP) derivative, **2-DMAP** ( $\delta_{11\text{B}}$  = –10.6 ppm, broad), the synthesis had to be carried out in THF as treatment of **1** with one equivalent of DMAP in benzene resulted in the formation of the bis(DMAP) adduct **3-DMAP** ( $\delta_{11\text{B}}$  = 4.2 ppm, Scheme 1b), in which the second DMAP equivalent has promoted a typical 1,2-migration of one hydrogen atom from boron to the CAAC<sup>Me</sup> ligand.<sup>26</sup> The solid-state structure of **3-DMAP** (Fig. 2) evidences the binding of the DMAP residues and the migration of H1 to C1, which is now sp<sup>3</sup>-hybridised (B1–C1 1.619(4), C1–N1 1.490(3) Å). In contrast, the binding of a second equivalent of pyridine to **2-Pyr** ( $\delta_{11\text{B}}$  = –9.3 ppm,

<sup>a</sup>Institut für Anorganische Chemie, Julius-Maximilians-Universität Würzburg, Am Hubland, 97074 Würzburg, Germany. E-mail: h.braunschweig@uni-wuerzburg.de

<sup>b</sup>Institute for Sustainable Chemistry & Catalysis with Boron, Julius-Maximilians-Universität Würzburg, Am Hubland, 97074 Würzburg, Germany

<sup>c</sup>Institut für Physikalische und Theoretische Chemie, Julius-Maximilians-Universität Würzburg, Emil-Fischer-Straße 42, 97074 Würzburg, Germany

† Electronic supplementary information (ESI) available: Synthetic procedures, NMR, EPR, UV-vis, IR, CV, X-ray crystallographic data and details of the computational analyses. CCDC 1956847–1956854. For ESI and crystallographic data in CIF or other electronic format see DOI: 10.1039/c9sc05026d

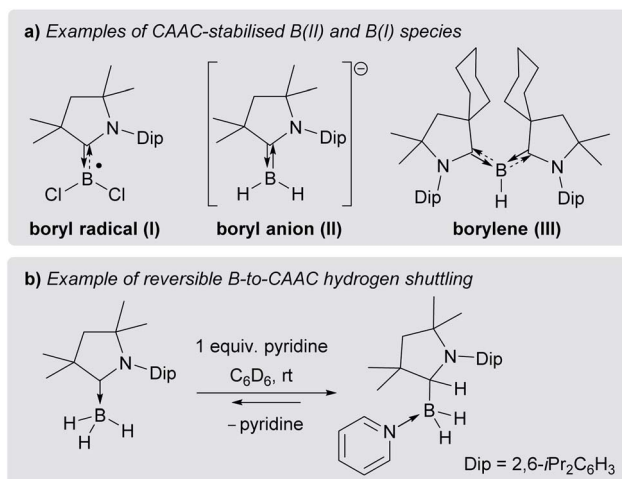
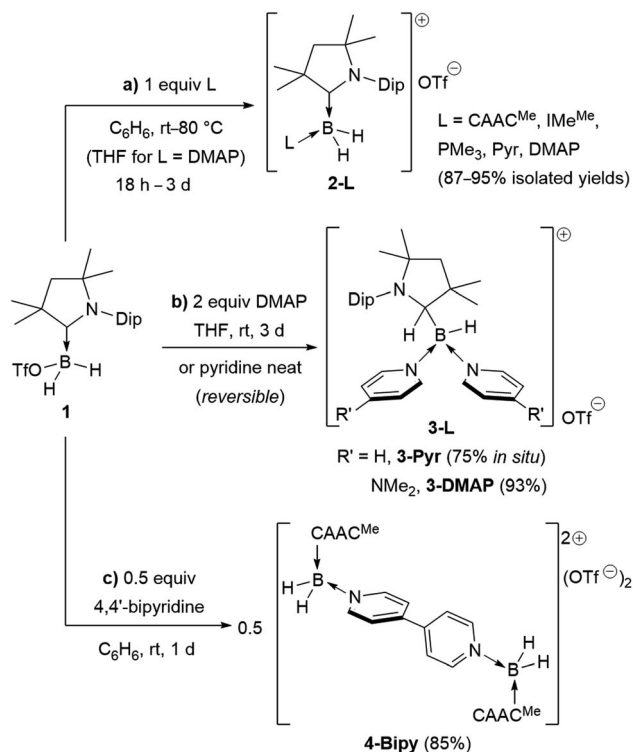


**Fig. 1** (a) Selected examples of CAAC-stabilised B(II) and B(I) species; (b) example of reversible Lewis-base-induced B-to-CAAC hydrogen shuttling.

broad) was found to be reversible: even in neat pyridine only *ca.* 75% conversion to **3-Pyr** ( $\delta_{11\text{B}} = 6.9$  ppm) was observed. The use of 4,4'-bipyridine as a base led to the formation of the 4,4'-bipyridine-bridged bis(boronium) species **4-Bipy** ( $\delta_{11\text{B}} = -8.6$  ppm, broad, Scheme 1c). Attempts to synthesise the derivative **2-thf** in THF resulted in ring-opening polymerisation of the solvent within two days at room temperature.



**Scheme 1** Syntheses of bis- and tris(base)-stabilised boronium cations (a) **2-L**, (b) **3-L** and (c) **4-L**. Isolated yields in brackets. IMe<sup>Me</sup> = 1,3,4,5-tetramethylimidazol-2-ylidene, Pyr = pyridine, DMAP = 4-dimethylaminopyridine.

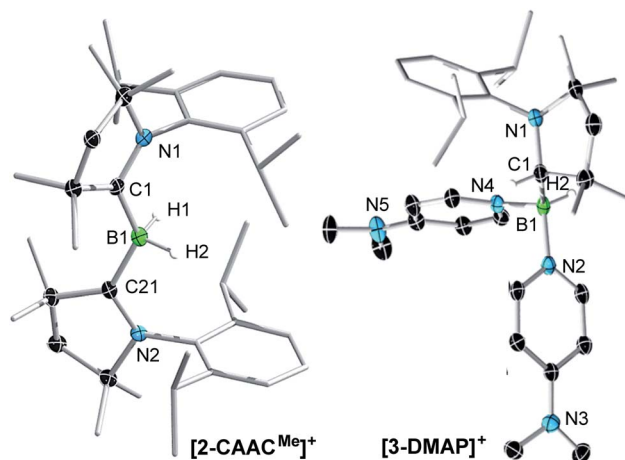
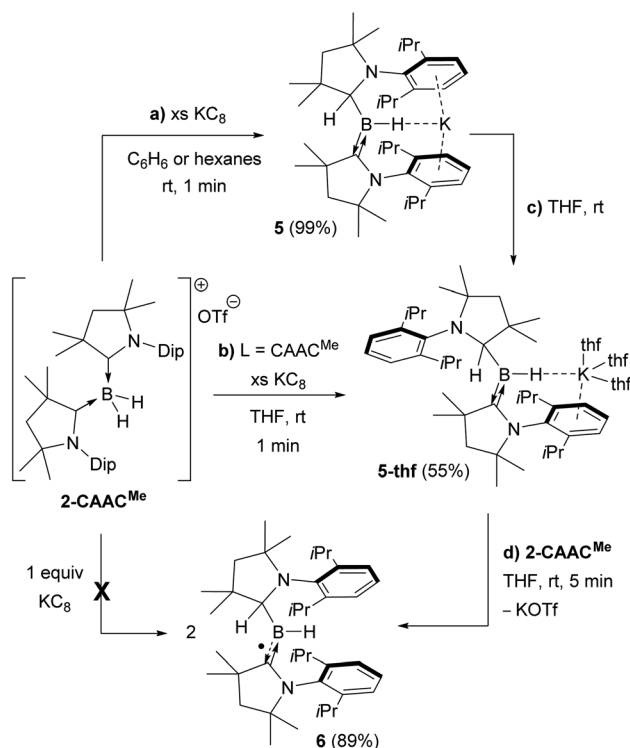


**Fig. 2** Crystallographically derived molecular structures of the **2-CAAC<sup>Me</sup>** (one of the two crystallographically distinct cations present in the asymmetric unit) and **3-DMAP** cations. Atomic displacement ellipsoids are set at 50% probability. Ellipsoids of CH<sub>3</sub> and *i*Pr groups, triflate counteranion and hydrogen atoms omitted for clarity except for boron-bound hydrides.† Selected bond lengths (Å) for **2-CAAC<sup>Me</sup>**: B1–C1 1.597(7), B1–C21 1.607(7), B1–H1 1.11(6), B1–H2 1.16(6), C1–N1 1.316(6), C21–N2 1.310(6); for **3-DMAP** B1–C1 1.619(4), B1–N2 1.585(3), B1–N4 1.597(3), B1–H2 1.10(2), C1–N1 1.490(3).

Attempts to reduce **2-L**, **3-L** and **4-L** under various conditions all resulted in unselective reactions, except for **2-CAAC<sup>Me</sup>**, which was readily reduced with excess KC<sub>8</sub> to the red-coloured (alkyl) hydroboryl anion **5** by 1,2-migration of one hydrogen atom from boron to CAAC<sup>Me</sup> (Scheme 2a). The <sup>11</sup>B NMR spectrum of **5**



**Scheme 2** Reduction of **2-CAAC<sup>Me</sup>** to boryl anions (a) **5** and (b)–(c) **5-thf**, and subsequent comproportionation to (d) boryl radical **6**.

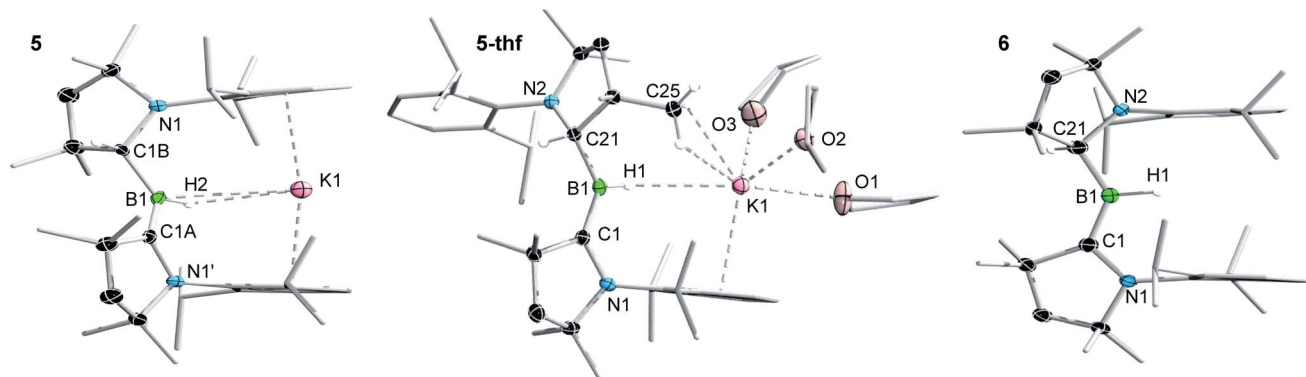


Fig. 3 Crystallographically derived molecular structures of **5**, **5-thf** and **6**. Atomic displacement ellipsoids are set at 50% probability. Ellipsoids of  $\text{CH}_2$ ,  $\text{CH}_3$  and  $\text{iPr}$  groups and hydrogen atoms omitted for clarity except for boron-bound hydrides.† Selected bond lengths (Å) and angles ( $^\circ$ ) for **5**: B1–C1A 1.439(11), B1–C1B 1.633(9), B1–H2 1.14(3), C1A–N1' 1.450(7), C1B–N1 1.520(8), K1...H1 2.53(3), K1...B1 3.141(4), K1...centroid 2.91,  $\Sigma \angle$  B1 359.4(12),  $\Sigma \angle$  C1A 359.7(5), B1–H2–K1 111.8(12); for **5-thf**: B1–C1 1.452(2), B1–C21 1.620(2), B1–H1 1.159(17), C1–N1 1.4601(18), C21–N2 1.5076(19), K1...H1 2.653(16), K1...B1 3.599(2), K1...centroid 2.95, K1...C25 3.2933(17),  $\Sigma \angle$  B1 359.9(1),  $\Sigma \angle$  C1 359.9(1), B1–H1–K1 138(1); for **6**: B1–C1 1.5174(18), B1–C21 1.5817(18), B1–H1 1.142(18), C1–N1 1.3777(15), C21–N2 1.4616(15),  $\Sigma \angle$  B1 359.5(6),  $\Sigma \angle$  C1 359.6(1).

shows a single broad resonance at 16.7 ppm, significantly downfield-shifted from that of other CAAC-stabilised boryl anions, which range from  $\delta_{\text{B}} = -4.7$  ppm for  $[(\text{CAAC}^{\text{Me}})\text{BH}_2]^-$  to  $\delta_{\text{B}} = -17.9$  ppm for  $[(\text{CAAC}^{\text{Cy}})\text{B}(\text{CN})_2]^-$ ,<sup>14–17</sup> likely because of the electron-withdrawing nature of the aminoalkyl substituent  $\text{CAAC}^{\text{MeH}}$ . The  $^1\text{H}\{^{11}\text{B}\}$  NMR spectrum shows a BH doublet at 1.90 ppm ( $J = 6.6$  Hz), coupling to the BCH resonance of the  $\text{CAAC}^{\text{MeH}}$  ligand at 4.38 ppm, as well as two sets of unsymmetrical  $\text{CAAC}^{\text{Me}}$  ligand resonances. An X-ray crystallographic analysis revealed a monomeric structure with a trigonal-planar boron atom ( $\Sigma \angle \text{B1 } 359(1)^\circ$ ), in which the potassium cation bound to the BH hydride (K1...H2 2.53(3) Å) is encapsulated by the ligand sphere through  $\eta^6$ - $\pi$  interactions with the Dip (=2,6-diisopropylphenyl) substituents of the  $\text{CAAC}^{\text{Me}}$  and  $\text{CAAC}^{\text{MeH}}$  ligands (Fig. 3). The B1–C1A bond length of 1.439(11) Å is significantly shorter than in the **2-CAAC<sup>Me</sup>** precursor (B–C<sub>avg</sub>, 1.69 Å, Fig. 2) and typical of a B=C double bond. This is indicative of strong  $\pi$  backdonation from the lone pair of the boryl anion to the  $\pi$ -accepting  $\text{CAAC}^{\text{Me}}$  ligand, as found in all CAAC-stabilised boryl anions.<sup>6,14–17</sup> According to DFT calculations carried out at the  $\omega\text{B97XD}/6\text{-}31+\text{G}^*$  level of theory, the HOMO of **5** possesses  $\pi$ -bonding character between B1 and C1A, with a nodal plane located at the C1A–N1' bond region (Fig. 4). As in **3-DMAP**, a 1,2-hydride shift has occurred and C1B is now  $\text{sp}^3$ -hybridised (B1–C1B 1.633(9), N1–C1B 1.520(8) Å). The presence of the hydrogen atom at boron was further confirmed by a solid-state infrared absorption at  $2329\text{ cm}^{-1}$ , corresponding to the B–H stretching mode. The computed B–H stretching mode of  $2352\text{ cm}^{-1}$  at  $\omega\text{B97XD}/6\text{-}31+\text{G}^*$  agrees well with the experimental value.

The reduction of **2-CAAC<sup>Me</sup>** in THF or the dissolution of **5** in THF both yielded the analogue **5-thf** (Scheme 2b, c and Fig. 3), in which the hydride-bound potassium cation is  $\eta^6$ - $\pi$ -stabilised now only by the Dip substituent of the neutral  $\text{CAAC}^{\text{Me}}$  ligand, its coordination sphere being completed by three THF molecules and an agostic interaction with one of the vicinal methyl groups (C25) of the  $\text{CAAC}^{\text{MeH}}$  ligand. The bond lengths and

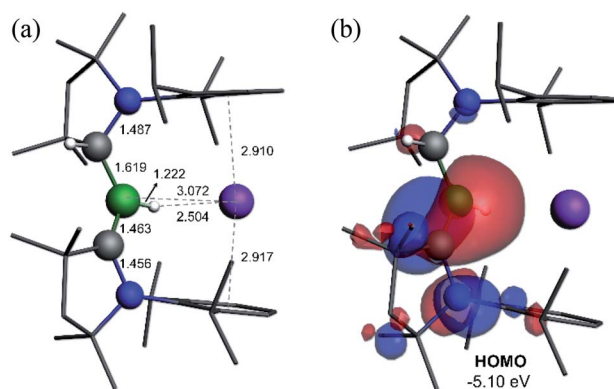


Fig. 4 (a) Calculated structure of **5** at the  $\omega\text{B97XD}/6\text{-}31+\text{G}^*$  level of theory. (b) Plot of the HOMO of **5** ( $\omega\text{B97XD}/6\text{-}311++\text{G}^{**}$ ).

angles of the boryl anion core change little compared to those of solvent-free **5**, the major difference being the conformation of the pyrrolidine rings of  $\text{CAAC}^{\text{MeH}}$  and  $\text{CAAC}^{\text{Me}}$ , which flip so that the Dip substituents now point in opposite directions.

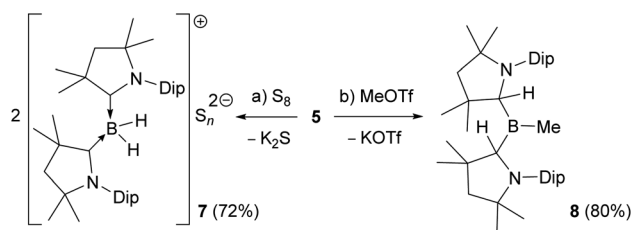
Cyclic voltammograms of **2-CAAC<sup>Me</sup>** and **5-thf** in THF (0.1 M  $[\text{nBu}_4\text{N}][\text{PF}_6]$ ) were essentially identical, showing a reversible redox event at  $E_{1/2} = -2.31$  V and an irreversible oxidation around  $-0.90$  V (relative to  $\text{Fc}/\text{Fc}^+$ ), suggesting that chemical oxidation of **5** to **6** should be possible. Indeed, the reaction of **5-thf** with **2-CAAC<sup>Me</sup>** led to quantitative disproportionation to the boryl radical **6** (Scheme 2d). Attempts to generate **6** by the direct one-electron reduction of **2-CAAC<sup>Me</sup>** failed, resulting instead in incomplete consumption of **2-CAAC<sup>Me</sup>** and generating a mixture of **5** and **6**. Radical **6** is deep purple in solution ( $\lambda_{\text{max}} = 523$  nm in the UV-vis spectrum) and  $^{11}\text{B}$  NMR-silent. In the solid state, however, isolated crystals of **6** are deep orange. X-ray diffraction analysis showed a structure very similar to **5** bar the potassium cation, with a trigonal planar B1 centre ( $\Sigma \angle \text{B1 } 359.5(6)^\circ$ ) and the Dip groups of the  $\text{CAAC}^{\text{MeH}}$  and  $\text{CAAC}^{\text{Me}}$  ligands both pointing in the same direction (Fig. 3).



Unlike in **5** and **5-thf**, the B1–C1 and C1–N1 bonds at the neutral CAAC<sup>Me</sup> ligand (1.5174(18) and 1.4601(18) Å, respectively) are within the range typical of partial double bonds, as is typical for CAAC-stabilised boryl radicals due to the delocalisation of the unpaired electron over the N1–C1–B1  $\pi$  framework.<sup>5–9,21,22,31–33</sup>

The IR spectrum of **6** shows a B–H stretching band at 2533 cm<sup>−1</sup> (calc.: 2558 cm<sup>−1</sup> at  $\omega$ B97XD/6-31+G\*), ca. 200 wavenumbers higher than that in **5**, and 100 higher than in Bertrand's hydroborylene **III** (Fig. 1a,  $\nu(\text{B–H}) = 2455 \text{ cm}^{-1}$ ), suggesting a significant strengthening of the B–H bond in radical **6**. The EPR spectrum of **6** displays a broad triplet from the hyperfine coupling to the <sup>14</sup>N nucleus ( $a_{\text{N}} = 18.5 \text{ MHz}$ , Fig. 5a). The simulated spectrum further provides hyperfine coupling parameters to the quadrupolar <sup>11</sup>B nucleus ( $a_{\text{B}} = 9.7 \text{ MHz}$ ), which is responsible for the line-broadening, and the BH and CAAC<sup>Me</sup>H <sup>1</sup>H nuclei ( $a_{\text{H}} = 13.6$  and  $4.8 \text{ MHz}$ , respectively). The presence of two distinct couplings to these <sup>1</sup>H nuclei suggests that the compound displays no fluxional B-to-CAAC hydrogen migration in solution.

Calculations show that the SOMO consists mainly of the B1–C1  $\pi$  bond with some  $\pi$ -antibonding character on the C1–N1 bond (Fig. 5c). The calculated Mulliken atomic spin densities are 53% on C1, 21% on N1 and only 15% on B1, showing that the unpaired electron is mainly delocalised on the CAAC ligand (Fig. 5d), as already suggested by the much stronger EPR hyperfine coupling to N1 than B1 (*vide supra*). To our knowledge, **6** is the first example of a neutral, structurally characterised hydroboryl radical. Moreover, to our surprise, isolated



Scheme 3 (a) Reducing and (b) nucleophilic reactivity of boryl anion **5**.

crystals of **6** proved air-stable at room temperature over a period of one week, making this compound a rare example of an air-stable boron-centred radical. This is presumably owed to a combination of the high degree of spin delocalisation, the low spin density at boron and the very effective encapsulation of the B–H unit by the CAAC<sup>Me</sup> and CAAC<sup>Me</sup>H ligands as seen in the electrostatic potential map in Fig. 5b. The only other air-stable boron-based radical reported is a permethylated icosahedral borane [*clos*-B<sub>12</sub>(CH<sub>3</sub>)<sub>12</sub>]<sup>•−</sup> radical anion, in which the unpaired electron is trapped and delocalised within the B<sub>12</sub> cage.<sup>34</sup>

Reactions of the boryl anion **5** with a wide range of electrophiles including haloboranes, organohalides, heavier group 14 chlorides, as well as Zn(II), Cu(I) and Au(I) halides all resulted in quantitative oxidation of **5** to radical **6**, and reduction of the corresponding electrophile. This contrasts with the boron nucleophile behaviour observed for CAAC-stabilised cyanoboryl anions.<sup>16,17</sup> With elemental sulfur, double oxidation back to the 2-CAAC<sup>Me</sup> cation was observed by NMR spectroscopic analysis ( $\delta_{\text{B}} = -22.4 \text{ ppm}$ ,  $t$ ,  $^1J_{\text{B}^{2-}\text{H}} = 84.7 \text{ Hz}$ ), the counteranion presumably being a S<sub>n</sub><sup>2−</sup> polysulfide (**7**, Scheme 3a). The only nucleophilic reactivity observed was with methyl triflate, which yielded clean salt metathesis to the methylated trialkylborane **8** through migration of the second hydride to the remaining CAAC<sup>Me</sup> ligand ( $\delta_{\text{B}} = 93.9 \text{ ppm}$ , Scheme 3b).

## Conclusions

We have shown herein that the ability of CAACs to stabilise electron-rich boron centres and reversibly activate B–H bonds can be harnessed together to reduce a [L<sub>2</sub>BH<sub>2</sub>]<sup>+</sup> cation to a [LRBH]<sup>•−</sup> anion without the usual need for halide abstraction, thanks to B-to-CAAC hydrogen shuttling. This boryl anion reacts principally as a one-electron reducing agent to yield the neutral hydroboryl radical [LRBH]<sup>•</sup>, the surprising stability of which is ensured by the unique stereoelectronic properties of the two encapsulating CAAC<sup>Me</sup> ligands.

## Conflicts of interest

The authors declare no conflict of interest.

## Acknowledgements

The authors thank the Deutsche Forschungsgemeinschaft for financial support. S. H. is grateful for a doctoral fellowship from

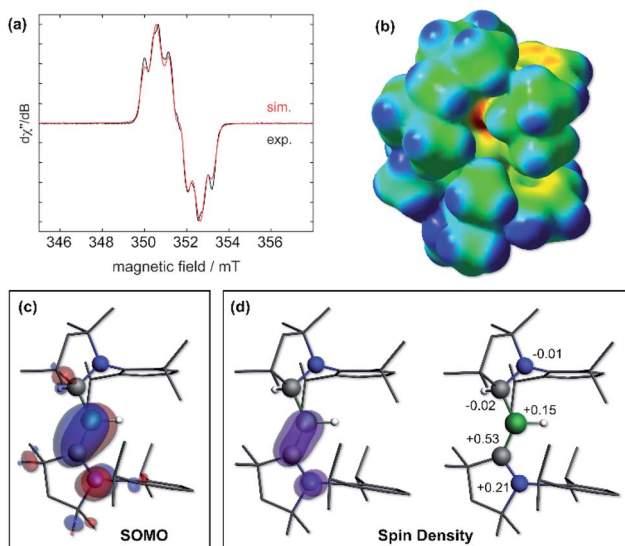


Fig. 5 (a) Experimental (black solid line) and simulated (red line) continuous-wave X-band EPR spectra of **6** in hexane solution at rt. Simulation parameters:  $g_{\text{iso}} = 2.0027$ ,  $a(^{11}\text{B}) = 9.7 \text{ MHz}$ ,  $a(^{14}\text{N}) = 18.5 \text{ MHz}$ ,  $a(^1\text{H}_{\text{H1}}) = 13.6 \text{ MHz}$  and  $a(^1\text{H}_{\text{H21}}) = 4.8 \text{ MHz}$ ; (b) electrostatic potential (ESP) map of **6** at the  $\omega$ B97XD/6-31+G\* level of theory. ESP charges following the notation of Fig. 3: N2:  $-0.46$ , C21:  $-0.01$ , B1:  $+0.19$ , H1:  $-0.17$ , C1:  $-0.27$ , N1:  $-0.14$ . (c) Plot of the SOMO of **6** (surface isovalue:  $\pm 0.03 [e a_0^{-3}]^{1/2}$ ). (d) Left: plot of the calculated spin density of **6** (surface isovalue:  $0.005 [e a_0^{-3}]$ ). Right: Mulliken atomic spin densities.





the Studienstiftung des Deutschen Volkes. F. F. thanks the Coordenação de Aperfeiçoamento de Pessoal de Nível Superior (CAPES) and the Alexander von Humboldt (AvH) Foundation for a Capes-Humboldt postdoctoral fellowship.

## Notes and references

‡ The boron-bound hydrides of each structure were detected as residual electron density in the difference Fourier map and freely refined.

§ The X-ray crystallographically-determined structures of **1**, **2-Pyr** and **2-DMAP** can be found in the ESI, Fig. S55–S57.†

- S. Kundu, S. Sinhababu, V. Chandrasekhar and H. W. Roesky, *Chem. Sci.*, 2019, **10**, 4727.
- U. S. D. Paul, M. J. Krahfuß and U. Radius, *Chem. Unserer Zeit*, 2018, **53**, 212.
- M. Melaimi, R. J. M. Soleilhavoup and G. Bertrand, *Angew. Chem., Int. Ed.*, 2017, **56**, 10046.
- M. Soleilhavoup and G. Bertrand, *Acc. Chem. Res.*, 2015, **48**, 256.
- Y. Su and R. Kinjo, *Coord. Chem. Rev.*, 2017, **352**, 346.
- M. Arrowsmith, J. I. Schweizer, M. Heinz, M. Härterich, I. Krummenacher, M. C. Holthausen and H. Braunschweig, *Chem. Sci.*, 2019, **10**, 5095.
- H. Braunschweig, I. Krummenacher, M.-A. Légaré, A. Matler, K. Radacki and Q. Ye, *J. Am. Chem. Soc.*, 2017, **139**, 1802.
- F. Dahcheh, D. Martin, D. W. Stephan and G. Bertrand, *Angew. Chem., Int. Ed.*, 2014, **53**, 13159.
- P. Bissinger, H. Braunschweig, A. Damme, I. Krummenacher, A. K. Phukan, K. Radacki and S. Sugawara, *Angew. Chem., Int. Ed.*, 2014, **53**, 7360.
- J.-S. Huang, W.-H. Lee, C.-T. Shen, Y.-F. Lin, Y.-H. Liu, S.-M. Peng and C.-W. Chiu, *Inorg. Chem.*, 2016, **55**, 12427.
- S. Kumar Sarkar, M. M. Siddiqui, S. Kundu, M. Ghosh, J. Kretsch, P. Stollberg, R. Herbst-Irmer, D. Stalke, C. Stückl, B. Schwederski, W. Kaim, S. Ghorai, E. D. Jemmis and H. W. Roesky, *Dalton Trans.*, 2019, **48**, 8551.
- D. A. Ruiz, M. Melaimi and G. Bertrand, *Chem. Commun.*, 2014, **50**, 7837.
- R. Kinjo, B. Donnadieu, M. A. Celik, G. Frenking and G. Bertrand, *Science*, 2011, **333**, 610.
- M. Arrowsmith, J. D. Mattock, S. Hagspiel, I. Krummenacher, A. Vargas and H. Braunschweig, *Angew. Chem., Int. Ed.*, 2018, **57**, 15272.
- M. Arrowsmith, J. D. Mattock, J. Böhnke, I. Krummenacher, A. Vargas and H. Braunschweig, *Chem. Commun.*, 2018, **54**, 4669.
- M. Arrowsmith, D. Auerhammer, R. Bertermann, H. Braunschweig, M. A. Celik, J. Erdmannsdörfer, I. Krummenacher and T. Kupfer, *Angew. Chem., Int. Ed.*, 2017, **56**, 11263.
- D. A. Ruiz, G. Ung, M. Melaimi and G. Bertrand, *Angew. Chem., Int. Ed.*, 2013, **52**, 7590.
- J. Böhnke, M. Arrowsmith and H. Braunschweig, *J. Am. Chem. Soc.*, 2018, **140**, 10368.
- M. Arrowsmith, D. Auerhammer, R. Bertermann, H. Braunschweig, G. Bringmann, M. A. Celik, R. D. Dewhurst, M. Finze, M. Grüne, M. Hailmann, T. Hertle and I. Krummenacher, *Angew. Chem., Int. Ed.*, 2016, **55**, 14462.
- M. Soleilhavoup and G. Bertrand, *Angew. Chem., Int. Ed.*, 2017, **56**, 10282.
- M.-A. Légaré, M. Rang, G. Bélanger-Chabot, J. I. Schweizer, I. Krummenacher, R. Bertermann, M. Arrowsmith, M. C. Holthausen and H. Braunschweig, *Science*, 2019, **363**, 1329.
- M.-A. Légaré, G. Bélanger-Chabot, R. D. Dewhurst, E. Welz, I. Krummenacher, B. Engels and H. Braunschweig, *Science*, 2018, **359**, 896.
- M.-A. Légaré, C. Pranckevicius and H. Braunschweig, *Chem. Rev.*, 2019, **119**, 8231.
- C. Hering-Junghans, *Angew. Chem., Int. Ed.*, 2018, **57**, 6738.
- A. J. Ruddy, D. M. C. Ould, P. D. Newman and R. L. Melen, *Dalton Trans.*, 2018, **47**, 10377.
- D. Auerhammer, M. Arrowsmith, H. Braunschweig, R. D. Dewhurst, J. O. C. Jiménez-Halla and T. Kupfer, *Chem. Sci.*, 2017, **8**, 7066.
- M. Arrowsmith, J. Böhnke, H. Braunschweig and M. A. Celik, *Angew. Chem., Int. Ed.*, 2017, **56**, 14287.
- S. Würtemberger-Pietsch, H. Schneider, T. B. Marder and U. Radius, *Chem. –Eur. J.*, 2016, **22**, 13032.
- M. R. Momeni, E. Rivard and A. Brown, *Organometallics*, 2013, **32**, 6201.
- G. D. Frey, J. D. Masuda, B. Donnadieu and G. Bertrand, *Angew. Chem., Int. Ed.*, 2010, **49**, 9444.
- A. Deisenberger, E. Welz, R. Drescher, I. Krummenacher, R. D. Dewhurst, B. Engels and H. Braunschweig, *Angew. Chem., Int. Ed.*, 2019, **58**, 1842.
- J. Böhnke, T. Dellermann, M. A. Celik, I. Krummenacher, R. D. Dewhurst, S. Demeshko, W. C. Ewing, K. Hammond, M. Heß, E. Bill, E. Welz, M. Röhr, R. Mitrić, B. Engels, F. Meyer and H. Braunschweig, *Nat. Commun.*, 2018, **9**, 1197.
- M. Arrowsmith, J. Böhnke, H. Braunschweig, M. A. Celik, C. Claes, W. C. Ewing, I. Krummenacher, K. Lubitz and C. Schneider, *Angew. Chem., Int. Ed.*, 2016, **55**, 11271.
- T. Peymann, C. B. Knobler and M. F. Hawthorne, *Chem. Commun.*, 1999, 2039.

